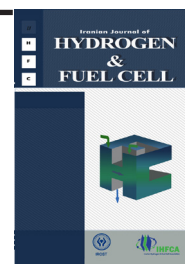


Iranian Journal of Hydrogen & Fuel Cell

IJHFC

Journal homepage://ijhfc.irost.ir



## Synthesis and electrochemical properties of $\text{Sr}_3\text{Fe}_{1.8}\text{Co}_{0.2}\text{O}_7$ as a solid oxide fuel cell cathode

Ayda Ghani Harzand<sup>1</sup>, Ali Nemat<sup>1\*</sup>, Mohammad Golmohammad<sup>2</sup>, Adrine Malek Khachatourian<sup>1</sup>

<sup>1</sup>Department of Materials Science and Engineering, Sharif University of Technology, Tehran, Iran

<sup>2</sup> Renewable Energy Department, Niroo Research Institute (NRI), Tehran, Iran

### Article Information

Article History:

Received:

04 Mar 2021

Received in revised form:

14 Apr 2021

Accepted:

17 Apr 2021

### Keywords

Solid oxide fuel cell  
Electrical conductivity  
Electrochemical behavior  
Ruddlesden-Popper  
Cathode

### Abstract

Solid oxide fuel cells (SOFCs) have attracted a lot of attention for their high efficiency, fuel flexibility, lower air pollution, etc. Unfortunately, their operating high temperature is the main shortcoming for commercialization. One of the main hurdles to achieving intermediate temperature SOFCs is the conductivity of their cathode materials at lower temperatures. Therefore, in this study, a conductive  $\text{Sr}_3\text{Fe}_{1.8}\text{Co}_{0.2}\text{O}_7$  cathode material with a Ruddlesden–Popper crystal structure was first successfully synthesized, and then the effect of sintering temperature was investigated. X-ray diffraction analysis results revealed that the powder was approximately pure. Moreover, field emission scanning electron microscope (FESEM) micrographs showed rod-shaped particles with an average particle size of 670 nm. To evaluate the sintering effect on the electrochemical behavior of the synthesized powder, a paste of the powder was painted on both sides of a Gadolinium doped Ceria (CGO) electrolyte and sintered at 1000°C and 1100°C. The electrochemical impedance analysis on symmetrical half-cells revealed that the minimum polarization resistance for the sintered cathode at 1000°C and 1100°C was 1.1  $\Omega\cdot\text{cm}^2$  and 1.6  $\Omega\cdot\text{cm}^2$  at 800°C. The FESEM micrograph showed High-temperature sintering could affect the interface between CGO and SFCO and decrease transport pathways for oxygen ions conduction at higher sintering temperatures. Also, the electrical conductivity of the sample was determined by the four-point probe electrical conductivity method in the temperature range of 200-800°C at room atmosphere. The results show that the maximum electrical conductivity at 427°C is 76  $\text{S}\cdot\text{cm}^{-1}$ .

## 1. Introduction

Solid oxide fuel cell (SOFC) technology is considered a promising approach to meet energy demand because

of its high conversion efficiency, low pollutant emission, and excellent fuel flexibility [1, 2]. However, its high operating temperature (~1000°C) leads to several issues, including interface reactions between

\*Corresponding author. nemati@sharif.edu  
Tel: 021-66165223 /Fax: 021-66005717

the cell components, poor durability, and high cost. Hence, a huge effort has been made to decrease the operating temperature to an intermediate temperature (IT) range of 500-800°C to enable the use of low-cost materials and improve long-term performance. Traditional cathode material, (La,Sr)MnO<sub>3</sub>, displays a low catalytic activity for the oxygen reduction reaction (ORR) below 800°C [3]. Current efforts are focused on developing new mixed ionic-electronic conductors (MIECs) for cathode materials with high electro catalytic activity for the ORR and good chemical and thermo-mechanical compatibility with other components in IT-SOFCs [4-6]. Extensive past works have been devoted to exploring suitable cathode materials to accelerate the ORR rate. Among those materials, Co-based perovskite or double perovskite materials, such as , , PrBaCo<sub>2</sub>O<sub>6-δ</sub>, and GdBaCo<sub>2</sub>O<sub>6-δ</sub>, have attracted the most attention because of their high catalytic activity toward oxygen dissociated adsorption reaction and their high oxygen ion conductivity, which greatly depresses the polarization resistances of the cells. However, the chemical stability of these materials at the operating conditions of the SOFCs is less attractive, leading to performance degradation during long-term operation [7].

As an alternative cathode material system, Ruddlesden-Popper (R-P) oxides with layered structures, especially the one-layered oxides of Pr<sub>2</sub>NiO<sub>4</sub>, La<sub>2</sub>NiO<sub>4</sub>, and La<sub>2</sub>CuO<sub>4</sub>, have gained special attention for their extremely high oxygen ion conductivities inside the rock salt layer. Although their catalytic activities toward ORR are not ideal, these R-P oxides provide useful information on the fundamental understanding of the transporting properties within their special structures [8, 9]. Recently, Sr<sub>3</sub>Fe<sub>2</sub>O<sub>7-δ</sub>, a double-layered oxide with two SrFeO<sub>3</sub> perovskite layers sandwiched by the SrO rock salt layers, came into the picture for its good oxygen and water storage capacity and high catalytic activity toward no decomposition. Unlike the formation of interstitial oxygen at the rock salt layer in A<sub>2</sub>BO<sub>4</sub> oxides, oxygen vacancies were reported to form at the intersection point of the two

perovskite layers, and protons are prone to form at the rock salt layer in a moisture atmosphere. In our recent work, we demonstrated SFO was an effective cathode in proton-conducting SOFCs, and the resulting performance was among one of the best so far [7].

With this perspective, the Ruddlesden-Popper (R-P) series of oxides, having a general formula (AO)(ABO<sub>3</sub>)<sub>n</sub> with n = 1, 2, and 3, have attracted attention as cathode materials for SOFC due to their mixed conducting properties [7, 10-12]. The R-P structure contains n repeating perovskite layers alternating with a rock-salt layer, and n = ∞ corresponds to the perovskite structure. Compared to the perovskite oxides, R-P phases usually exhibit improved structural stability without suffering from unwanted phase transitions [12, 13]. Co substitution in Sr<sub>n+1</sub>(Fe,Co)nO<sub>3n+1</sub> increases the electrical conductivity and catalytic activity for the ORR in IT-SOFCs [14, 15]. However, the thermal expansion coefficient (TEC) increases with Co substitution because of the low-spin to the high-spin transition of Co<sup>3+</sup> ions [15].

The structure of the n = 2 phase of the R-P oxide Sr<sub>3</sub>(Fe,Co)<sub>2</sub>O<sub>7-δ</sub> consists of two Sr(Fe,Co)O<sub>3</sub> perovskite layers alternating with a single SrO rock-salt layer along the c axis. This crystal structure is known to accommodate a considerable amount of oxygen non-stoichiometry 0 < δ < 1 without changing the crystal symmetry [16, 17]. Several compositions of this R-P phase with different substitutions in the A and B-site have been explored for oxygen separation membranes and SOFC cathode materials.

Therefore in this study, cobalt was partially doped into Sr<sub>3</sub>Fe<sub>2</sub>O<sub>7-δ</sub> using a polymerized complex method. Afterward, the prepared slurry of as-synthesized powders was applied on both sides of the Gadolinium doped Ceria (CGO) electrolyte. Then, the cathodes were sintered at two different temperatures to study the effect of sintering temperature. The electrochemical properties of the sample revealed that at 1000°C, the sintered cathode has better electrochemical properties.

## 2. Experimental

### 2.1. Materials and methods

$\text{Sr}_3\text{Fe}_{1.8}\text{O}_{7.8}$ : SFCO was synthesized by using the polymerized complex method. Iron nitrate nonahydrate  $\text{Fe}(\text{NO}_3)_3 \cdot 9\text{H}_2\text{O}$ , strontium carbonate  $\text{SrCO}_3$ , and nitrate cobalt ( $\text{Co}(\text{NO}_3)_2 \cdot 6\text{H}_2\text{O}$ ) were added to an aqueous solution of 333 mol citric acid (180 mL), and the resulting solution was stirred for 2 h at  $80^\circ\text{C}$  to solve the metal oxide complex. Ethylene glycol (333mmol) was added to the solution and stirred at  $130^\circ\text{C}$  for 4 h to produce a gelatinous solution. The gel was pyrolyzed in a mantle heater at  $350^\circ\text{C}$  for 3 h, and finally, the obtained brown powder was calcined at  $1000^\circ\text{C}$  for 5 h ( $\text{Sr}_3\text{Fe}_{1.8}\text{O}_{7.8}$ ) in an electronic furnace under a flow of air. It is worth mentioning that this temperature is the optimum one, and the expected crystal structure did not form at lower temperatures.

To measure the polarization resistance of the cathode, symmetrical half-cells were made with CGO electrolyte. To make a cathodic slurry, 1.6 gr of Ink Vehicle Terpeneol Based (VEH) was added to 1 gr of powder and placed in a ball mill for 24 hours. Then, the cathodic slurry was painted on both sides of the electrolyte (density: 99.5% and  $250\mu\text{m}$  in thickness) and sintered at two temperatures [18]. The silver paste was applied on both sides of the sintered cathode by painting on both sides of a symmetrical half-cell, then sintered at  $800^\circ\text{C}$  for 1 hour. The silver mesh was used as the current collector on both sides of the symmetrical half-cell.

To prepare the sample for the four-probe electrical conductivity test, the powder was uniaxially pressed (200 MPa) in a rectangular cube shape with approximate dimensions of  $20 \times 20 \times 2$  mm and sintered at  $1250^\circ\text{C}$  for 5 hours. To determine the electrical conductivity cathodic of the sample, the two outer surfaces of the part are coated as external electrodes for the entry of electric current by silver paste. Also, internal electrodes with a specific formula was developed for measuring potential drop by silver paste on the sample.

### 2.2. Characterization

X-ray diffraction (XRD) patterns were recorded using a PAN analytical (X'Pert PROMPD) using  $\text{Cu-K}_\alpha$  radiation over the angular range of  $20$ – $80^\circ$ . Field emission electron microscopy (FESEM, TeScan – Mira III) was used to evaluate the morphology of the synthesized powders and to determine their particle size. To obtain the polarization resistance of the cathode, the electrochemical impedance spectroscopy (EIS) of symmetrical half-cells with CGO electrolyte was performed by Auto-lab 320 in the temperature range of  $700$ – $800^\circ\text{C}$  and the frequency range of  $0.1$  Hz to  $10$  MHz. The electrical conductivity was determined by a digital four resistance ohmmeter (DUCTER DLRO-10) in the temperature range of  $200$ – $800^\circ\text{C}$  in the air.

## 3. Results and Discussion

Figure 1 shows the X-ray diffraction pattern of powder. The results show that the as-synthesize powder is a pure with the RP structure and crystallite size of  $399\text{\AA}$ . As can be seen, the addition of Co resulted in a shift of the peaks, which confirms the doping of the Co in the SFO structure.

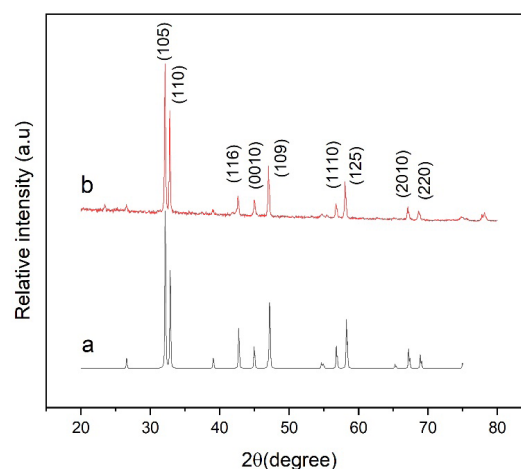


**Fig. 1.** X-Ray Diffraction patterns of a) SFO produced from the standard card and b) pure SFCO powder prepared by the polymerized complex method calcined at  $1000^\circ\text{C}$ .

The FESEM micrographs of calcined SFCO powder at 1000°C for 5 hours are shown in Figure 2. As can be seen, the particles are mostly sub-micron with an average particle size of 0.67 μm. Also, the shape of the powder is a rod.

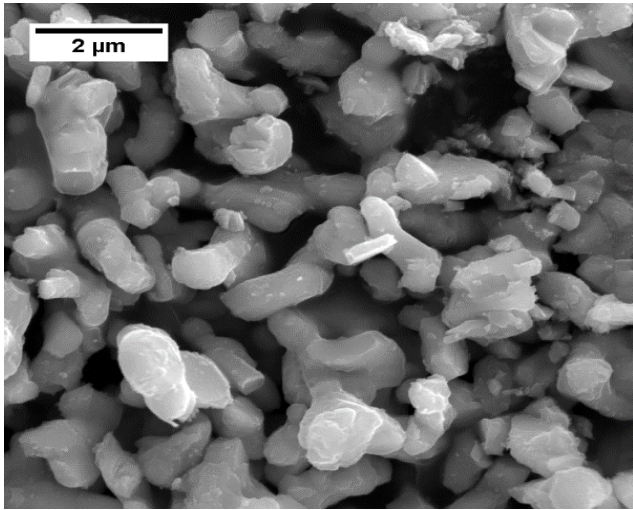


Fig.2. FESEM image of  $Sr_3Fe_{1.8}Co_{0.2}O_{7.6}$  calcined at 1000°C.

After applying the cathode layer to both sides of the CGO electrolyte, the resistance of the symmetric cells

was evaluated by alternating current impedance analysis to evaluate the electrochemical performance of the synthesized powder.

Figure 3 shows the Nyquist plots of samples sintered at different temperatures. The point of contact with the horizontal axis at high frequencies indicates the ohmic resistance, which includes the ionic resistance of the electrolyte, the electron resistance of the electrodes, and the resistors related to the junction. The intersection with the horizontal axis at low frequencies shows the total resistance. The difference between the total resistance and the ohmic resistance in symmetrical cells shows the polarization resistance created between the cathode surface and the electrolyte.

As expected, the polarization resistance between the cathode surface and the electrolyte decreases as the sintering temperature increased. Figure 3(a) shows the Impedance plot for SFCO sintered at 1000°C. The minimum polarization resistance for this compound was 1.1 at 800°C. As the temperature decreases, the polarization resistance increases and is 1.7 and 4.2 at 750°C and 700°C, respectively.

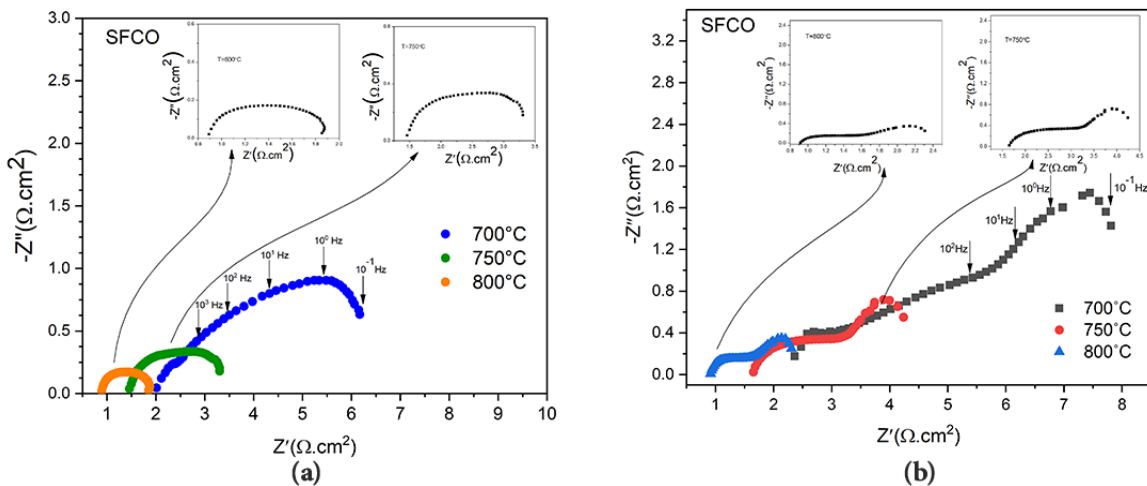


Fig.3. AC impedance spectra in the 700-800°C temperatures range and frequency from  $10^{-1}$  to  $10^3$  Hz for SFCO cathodes sintered at a) 1000°C and b) 1100°C.

Figure 3(b) shows the SFCO cathode impedance curve sintered at 1100 ° C. The polarization resistances in this sample at temperatures of 700 ° C, 750 ° C, and 800 ° C were measured as 5.6, 2.3, and 1.6, respective-

ly. Dao MingHuan and Zhiguanwag [19] researched SFCO, and their impedance resistance was reported at 500°C, 1.7. Karinjilottu et al. [20] reported lower polarization resistance for SLFCO, SNFCO, and SCLFCO

of 700, 750, and 800°C, respectively (see Table 1), because when Co was doped, the electrical conductivity and thermal expansion coefficient (TEC) increased.

**Table 1: Impedance resistance reported by Karinjilottu et al. [20].**

Name	700C	750C	800C
SLFCO	0.5	0.3	0.2
SCLFCO	0.6	0.1	0.05
SNFCO	0.56	0.33	0.21
SCNFCO	0.52	0.31	0.11

Figure 4 has shown an Arrhenius diagram of the polarization resistance of a sintered cathode at 1000°C and 1100°C in the 700-800°C temperature range. Sintered SFCO at 1100°C had the highest polarization resistance of all temperatures in the mentioned range. Sintering temperature has a strong effect on polarization resistance. As the sintering temperature was increased, the interface between CGO and SFCO, which provide fast transport pathways for oxygen ions conduction, could be severely destroyed. The excellent oxygen ion transport and improved catalytic activity toward the O<sub>2</sub> reduction reaction of SFCO should account for this enhancement.

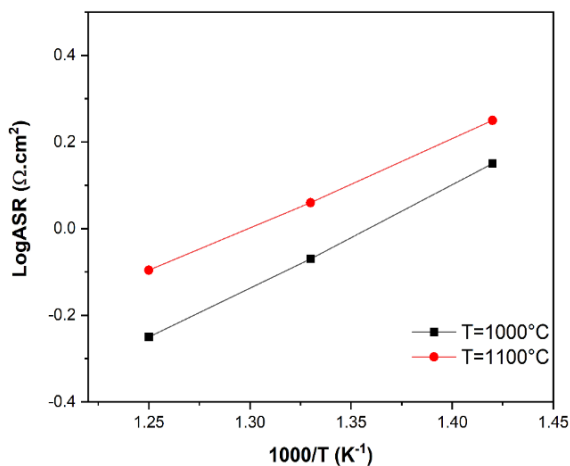


**Fig.4. Arrhenius diagram of the polarization resistance of sintered cathodes at 1000C and 1100C in the 700-800C temperature range.**

To better understand the electrical properties, the four-probe method was used to determine the electri-

cal conductivity of the cathode composition. In this method, the resistance of the samples was calculated by measuring the potential decreasing with a specific current, then the equation below was used to determine the electrical conductivity of the samples.

$$\sigma = \frac{1}{\rho} = \frac{L}{RA}$$

$\rho$ : Specific resistance

$\sigma$ : Electrical conductivity

A: Cross-section

L: The distance between the two electrodes

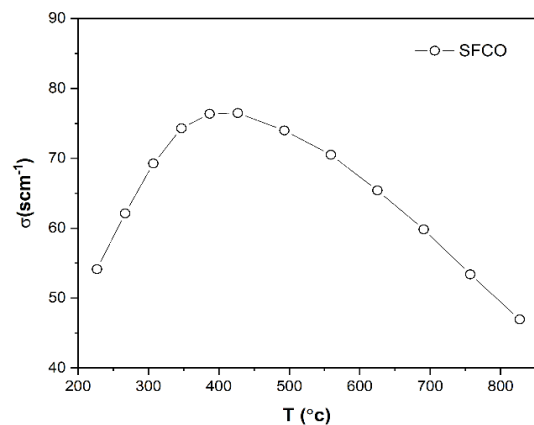


**Fig. 5. Electrical conductivity of the SFCO sample measured at various temperatures.**

Figure 5 shows the electrical conductivity changes of SFCO powders that were cold-pressed into a rectangular with 20 mm in height, 20 mm in length, and 20 mm in width after sintering at 1250°C for 5 h in air. The maximum amount of conductivity of an SFCO sample at 427°C is 76 S. The electrical conductivity of the compound first increases and then decreases with increasing temperature due to the law of semiconductors. As the temperature increases, the conductivity increases because the concentration of free electrons increases, but at a certain temperature, the conductivity decreases due to the reduced mobility of the free electrons.

Figure 6 shows  $\ln(\sigma T)$  per 1000/K for our cathodic sample. At low temperatures, the curve is linear which indicates that the conductivity via small-Polaron Hopping. Therefore, in this part, the activation energy of the polarization process is calculated by the relationship below [21, 22].

$$\ln(\sigma T) = \frac{-E_a}{RT} + \ln A$$

$\sigma$ : Conductivity

T: Temperature

$E_a$ : activation energy

A: Chemical constant

R: Universal Gas Constant

The activation energy for the sample in the linear part in the 300-400 temperature range is 1 eV. The activation energy for two crystal structures similar to the compounds used in this study, i.e., SCNFCO and SF-CMO, are 1.56eV and 1.1eV, respectively [20, 23].

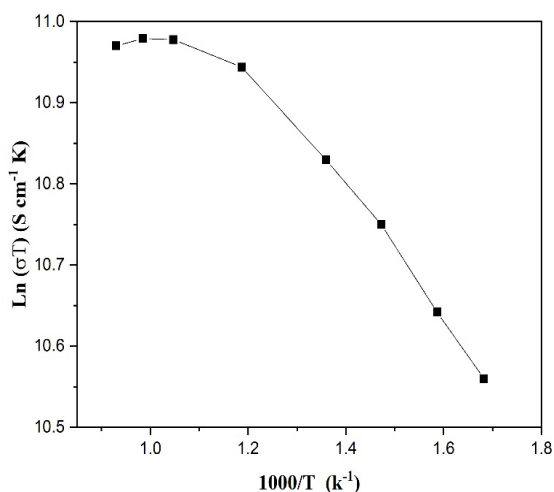


Fig. 6. Arrhenius diagram of the SFCO cathodic composition sintered at 1250 °C for 5 hours.

Figure 7(a) shows the cross-sectional area of a symmetrical half-cell SFCO cathode sintered at 1000 °C after electrochemical impedance analysis of the part

where silver was not applied. The cathode had good adhesion to the electrolyte, and no separation occurred between them. Also, due to the microstructure, uniform porosity was created in the cathode after the calcination operation. The cathodic layer applied to the electrolyte in the symmetrical half-cell has a uniform thickness. Figure 7(b) shows the separation that occurred between the cathode and electrolyte in a symmetrical half-cell SFCO cathode sintered at 1100 °C. Therefore, as the SEM images show, high-temperature sintering significantly decreases the interface area between the cathode layer and electrolyte, which can provide the ionic transport pathway. This work clearly shows how sintering temperature affects ionic conduction. We found that interfacial ionic conduction plays a central role in the CGO-SFCO fuel cell device performance.

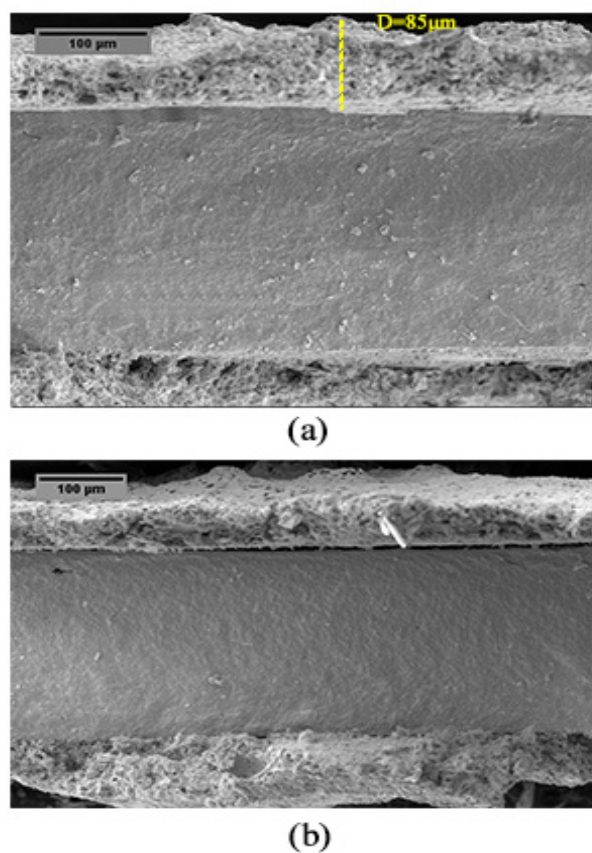


Fig.7. FESEM images of a fractured symmetric cell after testing SFCO cathodes sintered a) at 1000 °C and b) at 1100 °C.

## 4. Conclusions

In this study, an SFCO compound with a R-P2 crystal structure was successfully synthesized by a polymerized complex method. The XRD and FESEM results revealed that the powder was approximately pure and sub-micron in size. The electrical properties revealed that the maximum electrical conductivity of SFCO was 76 S. at 427°C. The reason for this behavior is the opposite interaction of the concentration and mobility of free electrons. Moreover, EIS results revealed that the sintering temperature has a significant impact on SFCO cathode polarization resistance, and as a result, conductivity. The minimum polarization resistance of SFCO sintered at 1000 ° C was obtained at 800 ° C with a value of 1.1, which is about 50% less than the sample sintered at 1100° C. This behavior might be due to the high-temperature sintering destroying the interface between CGO and SFCO, which provides fast transport pathways for oxygen ions conduction. The excellent oxygen ion transport and the improved catalytic activity toward the O<sub>2</sub> reduction reaction of SFCO should account for this enhancement.

## References

- [1]. Jacobson, A.J., Materials for solid oxide fuel cells. *Chemistry of Materials*, 2010. 22(3): p. 660-674.
- [2]. Steele, B.C. and A. Heinzel, Materials for fuel-cell technologies, in *Materials For Sustainable Energy: A Collection of Peer-Reviewed Research and Review Articles from Nature Publishing Group*. 2011, World Scientific. p. 224-231.
- [3]. Yamamoto, O., Solid oxide fuel cells: fundamental aspects and prospects. *Electrochimica Acta*, 2000. 45(15-16): p. 2423-2435.
- [4]. Sun, C., R. Hui, and J. Roller, Cathode materials for solid oxide fuel cells: a review. *Journal of Solid State Electrochemistry*, 2010. 14(7): p. 1125-1144.
- [5]. Manthiram, A., et al., Crystal chemistry and properties of mixed ionic-electronic conductors. *Journal of electroceramics*, 2011. 27(2): p. 93-107.
- [6]. Kilner, J.A. and M. Burriel, Materials for intermediate-temperature solid-oxide fuel cells. *Annual Review of Materials Research*, 2014. 44: p. 365-393.
- [7]. Huan, D., et al., High-performanced cathode with a two-layered R-P structure for intermediate temperature solid oxide fuel cells. *ACS Applied Materials & Interfaces*, 2016. 8(7): p. 4592-4599.
- [8]. Torabi, M., et al., Experimental investigation of a solid oxide fuel cell stack using direct reforming natural gas. *Iranian Journal of Hydrogen & Fuel Cell*, 2017. 4(4): p. 301-306.
- [9]. Ghorbani-Moghadam, T., et al., Characterization, Electrical and Electrochemical Study of La<sub>0.9</sub> Sr<sub>1.1</sub> Co<sub>1-x</sub> Mo<sub>x</sub> O<sub>4</sub> (x ≤ 0.1) as Cathode for Solid Oxide Fuel Cells. *Journal of Electronic Materials*, 2020. 49(11): p. 6448-6454.
- [10]. Armstrong, T., F. Prado, and A. Manthiram, Synthesis, crystal chemistry, and oxygen permeation properties of LaSr<sub>3</sub>Fe<sub>3-x</sub>Co<sub>x</sub>O<sub>10</sub> (0 ≤ x ≤ 1.5). *Solid state ionics*, 2001. 140(1-2): p. 89-96.
- [11]. Woolley, R.J. and S.J. Skinner, Novel La<sub>2</sub>NiO<sub>4+δ</sub> and La<sub>4</sub>Ni<sub>3</sub>O<sub>10-δ</sub> composites for solid oxide fuel cell cathodes. *Journal of power sources*, 2013. 243: p. 790-795.
- [12]. Kim, J.-H. and A. Manthiram, Characterization of Sr<sub>2</sub>.7Ln<sub>0.3</sub>Fe<sub>1.4</sub>Co<sub>0.6</sub>O<sub>7</sub> (Ln= La, Nd, Sm, Gd) intergrowth oxides as cathodes for solid oxide fuel cells. *Solid State Ionics*, 2009. 180(28-31): p. 1478-1483.
- [13]. Kim, J.-H., et al., Crystal chemistry and electrochem-

ical properties of Ln (Sr, Ca) <sub>3</sub> (Fe, Co) <sub>3</sub> O <sub>10</sub> intergrowth oxide cathodes for solid oxide fuel cells. *Journal of Materials Chemistry*, 2011. 21(8): p. 2482-2488.

[14]. Kim, Y. and A. Manthiram, Electrochemical properties of Ln (Sr, Ca) <sub>3</sub> (Fe, Co) <sub>3</sub> O <sub>10</sub>+ Gd<sub>0.2</sub>Ce<sub>0.8</sub>O<sub>1.9</sub> composite cathodes for solid oxide fuel cells. *Journal of The Electrochemical Society*, 2011. 158(10): p. B1206.

[15]. Lee, K. and A. Manthiram, LaSr<sub>3</sub>Fe<sub>3-y</sub>Co<sub>y</sub>O<sub>10-δ</sub> (0 ≤ y ≤ 1.5) Intergrowth Oxide Cathodes for Intermediate Temperature Solid Oxide Fuel Cells. *Chemistry of materials*, 2006. 18(6): p. 1621-1626.

[16]. Manthiram, A., F. Prado, and T. Armstrong, Oxygen separation membranes based on intergrowth structures. *Solid State Ionics*, 2002. 152: p. 647-655.

[17]. Markov, A.A., et al., Oxygen nonstoichiometry and ionic conductivity of Sr<sub>3</sub>Fe<sub>2-x</sub>Sc<sub>x</sub>O<sub>7-δ</sub>. *Chemistry of materials*, 2007. 19(16): p. 3980-3987.

[18]. Mohebbi, H., et al., The Effect of Process Parameters on the Apparent Defects of Tape-Cast SOFC Half-Cell. 2019. 5(4): p. 12-16.

[19]. Huan, D., et al., High-performanced cathode with a two-layered R–P structure for intermediate temperature solid oxide fuel cells. 2016. 8(7): p. 4592-4599.

[20]. Padmasree, K.P., et al., Electrochemical properties of Sr<sub>2.7-x</sub>CaxLn<sub>0.3</sub>Fe<sub>2-y</sub>CoyO<sub>7-δ</sub> cathode for intermediate-temperature solid oxide fuel cells. *International Journal of Hydrogen Energy*, 2019. 44(3): p. 1896-1904.

[21]. Kuo, J., H.U. Anderson, and D.M.J.J.o.S.S.C. Sparlin, Oxidation-reduction behavior of undoped and Sr-doped LaMnO<sub>3</sub> nonstoichiometry and defect structure. 1989. 83(1): p. 52-60.

[22]. Zhou, Q., et al., Novel cobalt-free cathode material (Nd<sub>0.9</sub>La<sub>0.1</sub>)<sub>2</sub>(Ni<sub>0.74</sub>Cu<sub>0.21</sub>Al<sub>0.05</sub>)O<sub>4+δ</sub> for inter-

mediate-temperature solid oxide fuel cells. 2015. 41(1): p. 639-643.

[23]. Zhao, Y., et al., Performance and distribution of relaxation times analysis of Ruddlesden-Popper oxide Sr<sub>3</sub>Fe<sub>1.3</sub>Co<sub>0.2</sub>Mo<sub>0.5</sub>O<sub>7-δ</sub> as a potential cathode for protonic solid oxide fuel cells. 2020. 352: p. 136444.